Proceedings of the Research Institute of Atmospherics,
Nagoya University, Vol. 36, No. 2 (1989)

THE EFFECTS OF THE MAJOR SOLAR STORM OF FEBRUARY 1986 AS SEEN BY ENERGETIC PARTICLE DETECTOR ON THREE NEARLY EQUIDISTANT GEOSYNCHRONOUS SATELLITES

R.D. Belian and T.E. Cayton

Los ALamos National Laboratory, Los Alamos, New Mexico 87545, U. S. A.

1. Introduction

In this report we describe in very general terms the great solar storm of February 1986 as recorded by the CPA detectors on three geosynchronous orbit satellites in energetic particles during February 7, 8, and 9. The entire period is characterized by large energetic particle enhancements, particle dropouts, and long periods during which the global energetic particle content of the magnetosphere appears to be at the strong pitch angle diffusion limit. The dropouts are due to excursions of one or more satellites into the lobe or magnetosheath due to compression of the magnetosphere. The two most dramatic effects are quasiperiodic flux variations and a long period during which the magnetopause was compressed to inside the geosynchronous orbit for ~4 hours.

2. Instrumentation

Electron and proton fluxes are measured with the low-energy-range electron (LoE) and low-energy-range proton (LoP) detectors of the Los Alamos Charged Particle Analyzer (CPA). This instrument has been flown aboard several geosynchronous orbit satellites, including the three spacecraft (S/C) from which the data presented here were obtained: S/C 1984–037 located near 70°E and about 9° below the magnetic equator, S/C 1984–129, located near 205°E and straddling the magnetic equator, and S/C 1982–019 located near 323°E and about 10° above the magnetic equator. (All three S/C were within 2° of the geographic equator.) Each S/C rotates with a nominal 10.2 s period about an axis that points radially inward toward the center of the earth. For more information about the CPA instrument see Higbie *et al.* [1978] and Baker *et al.* [1985].

The data presented here are five-minute averages (involving approximately 1200 individual measurements) of the integral flux in each of several energy channels. The low energy electrons are averaged from five look directions relative to the spin axis while the protons are averaged from a single look direction perpendicular to the spin axis.

Each LoE passband is defined by an upper cutoff and a threshold level. The LoE passbands plotted for all three spacecraft are given in Table I.

LoE Channel	Thresholds
E1	30 keV
E2	45 keV
E3	65 keV
E4	95 keV
E5	140 keV
E6	200 keV
Cutoff	300 keV

Table I. LoE Detector Energy Passbands

The LoP passbands are defined by an upper cutoff and a threshold level. The LoP passbands plotted for the three spacecraft are given in Table II.

LoP	1982–019	1984–037	1984–129
Channel	Thresholds	Thresholds	Thresholds
P1	95 keV	70 keV	72 keV
P3	130 keV	100 keV	104 keV
P5	195 keV	160 keV	153 keV
P7	255 keV	235 keV	235 keV
P9	380 keV	350 keV	365 keV
Cutoff	600 keV	560 keV	573 keV

Table II. LoP Detectors Energy Passbands

Universal time is indicated along the bottom of each graph; local time for each satellite is indicated along the top of the corresponding panel.

3. Observations

The data are presented on the six pages labeled 1a, 1b, 1c, and 2a, 2b, 2c, with 1a–c referring to electrons of the passbands given above and 2a–c referring to ion data. Each

page contains data for the three geosynchronous orbit satellites for one day. Universal time is shown on the ordinate of the bottom panel (curves for 1984–037), and the spacecraft local time is shown at the top of each panel. The upper curve of each panel represents data from the lowest energy passband and each succeeding curve is for higher and higher passbands. Referring to the figures we can pick out the following features:

a) Large increases in the ambient particle populations at one or more satellite, often in concert between the widely separated satellites, cf.~0500 UT, ~100 UT, and ~1700 UT all on February 7, 1986 (Figures 1a and 2a). Many more such events are observed on February 8, 1986 (Figures 1b and 2b). One might be tempted to consider these as injections in the classical sense, i.e., injection of newly energized particles in a discrete bunch near midnight from the tail, cf. Belian *et al.* 1978, and references. However, the simultaneity of the increases at widely separated satellites and the lack of appreciable energy dispersion in many of the enhancements (see the enhancement at ~2300 UT on 2/8/86) make that interpretation highly unlikely. For example, the drift period of 30 keV electrons in a dipolar field is ~3 hours, so that particles in a discrete bunch that pass the location of a given satellite would not be expected to drift to the location of the next satellite for about 1 hour. We observed enhancements in some event, (e.g., ~0500 UT on 2/8/86 Figures 2a and 2b) at all three satellites within ~10 minutes of each other.

b) Numerous dropouts of the energetic particle populations are observed i.e., at ~1650 UT on 2/7/86 (Figure 1a, in all 3 satellites, and at ~2120 UT in 1984–129 (Figure 1a), where the fluxes of electrons drop by 2–3 orders of magnitude in a few minutes. The dropouts occur for different reasons depending on the location of the satellite in its orbit. On the dayside from ~0800 LT to ~1600 LT, dropouts occur because the dynamic pressure of the solar wind compresses the magnetosphere until the magnetopause is inside the geosynchronous orbit and the satellite finds itself in the magnetosheath. For other local times the compression takes the satellites into the lobe regions of open field lines. A particularly significant compression occurred on 2/8/86 from ~2000 UT to ~2400 UT. This is seen in both the electron and ion fluxes for 1984–129 (Figures 1b and 2b), which happened to be on the dayside from 0930 to 1330 LT.

c) The period of time from ~0500 to~2200 UT on 2/8/86 in both electron and ion plots (Figures 1b and 2b) is very interesting. There were ~17 hours during which the electron fluxes at times approached or exceeded the empirically determined strong pitch angle diffusion limit for > 30 keV electron fluxes, determined by Baker *et al.* [1979]. During this highly compressed and excited state, the magnetosphere was able to maintain slightly higher populations of > 30 keV electrons for short periods than have been observed for other times (see Baker *et al.*, 1979). Another interesting aspect of this period is the quasiperiodic nature of the data, seen in both electron and protons but especially well in the low energy proton plots. Beginning at ~0500 UT there were 4 or 5 occurrences wherein the fluxes, after significant drops, rapidly increased by $\lesssim$, nearly simultaneously at all three

satellites, to values that exceeded the value seen before the drop. The increases were then followed by gradual declines in flux until they again rapidly increased back to approximately the same strong pitch angle diffusion limit to repeat the cycle. Cycle times were ~2 hours in duration. The process is nonadiabatic during the flux increase, at least for $\geq$ 30 keV electrons and $\geq$ 70 keV ions and heating is seen to occur in that the spectrum is seen to flatten. The process appears adiabatic during the flux decrease. What we may have observed here was that the rapid compression of the magnetosphere caused two effects: a) the compressed field caused particle populations from deeper within the trapping regions to nonadiabatically diffuse outward, thereby increasing the fluxes; b) the ambient particle populations were heated by the compression. The rapid increase was followed by the slower adiabatic loss of particles due to strong pitch angle scattering and/or other effects. The cycles continued until the process was interrupted by a substantial increase in the solar wind moments that gave rise to the 4–hour long highly compressed state that began at ~2000 UT. Why the process occurred several times quasiperiodically cannot be determined from this data alone; we are in the process of looking at other data sets in hopes they will shed some light on the subjects.

The authors thank Karla J. Sofaly for handling the CPA data and for producing the plots presented here. This work was performed under the auspices of the U. S. Department of Energy.

References

Baker, D.N., *et al.*, Los Alamos Energetic Particle Sensor System at Geostationary Orbit, *AIAA* 85–0243, 1985.

Baker, D.N., *et al.*, Strong electron pitch angle diffusion observed at geostationary orbit, *Geophys. Res. Lett.* 6, 205, 1979.

Higbie, P.R., R.D. Belian, and D.N. Baker, High-resolution particle measurements at 6.6 R_E: 1. Electron micropulsations, *J. Geophys. Res.*, 83, 4851, 1978.

Belian, R.D. *et al.*, High-resolution energetic particle measurements at 6.6 R_E: 2. High-energy proton drift echoes, *J. Geophys. Res.*, 83, 4857, 1978.

Figure Captions

Fig. 1a, 1b, 1c. Low-energy electron plots. Each panel contains six energy passbands from one of three geosynchronous orbit satellites. See Table I for the passbands.

Fig. 2a, 2b, 2c. Low-energy proton plots. Each panel contains five energy passbands from one of the three geosynchronous orbit satellites. See Table II for the passbands.

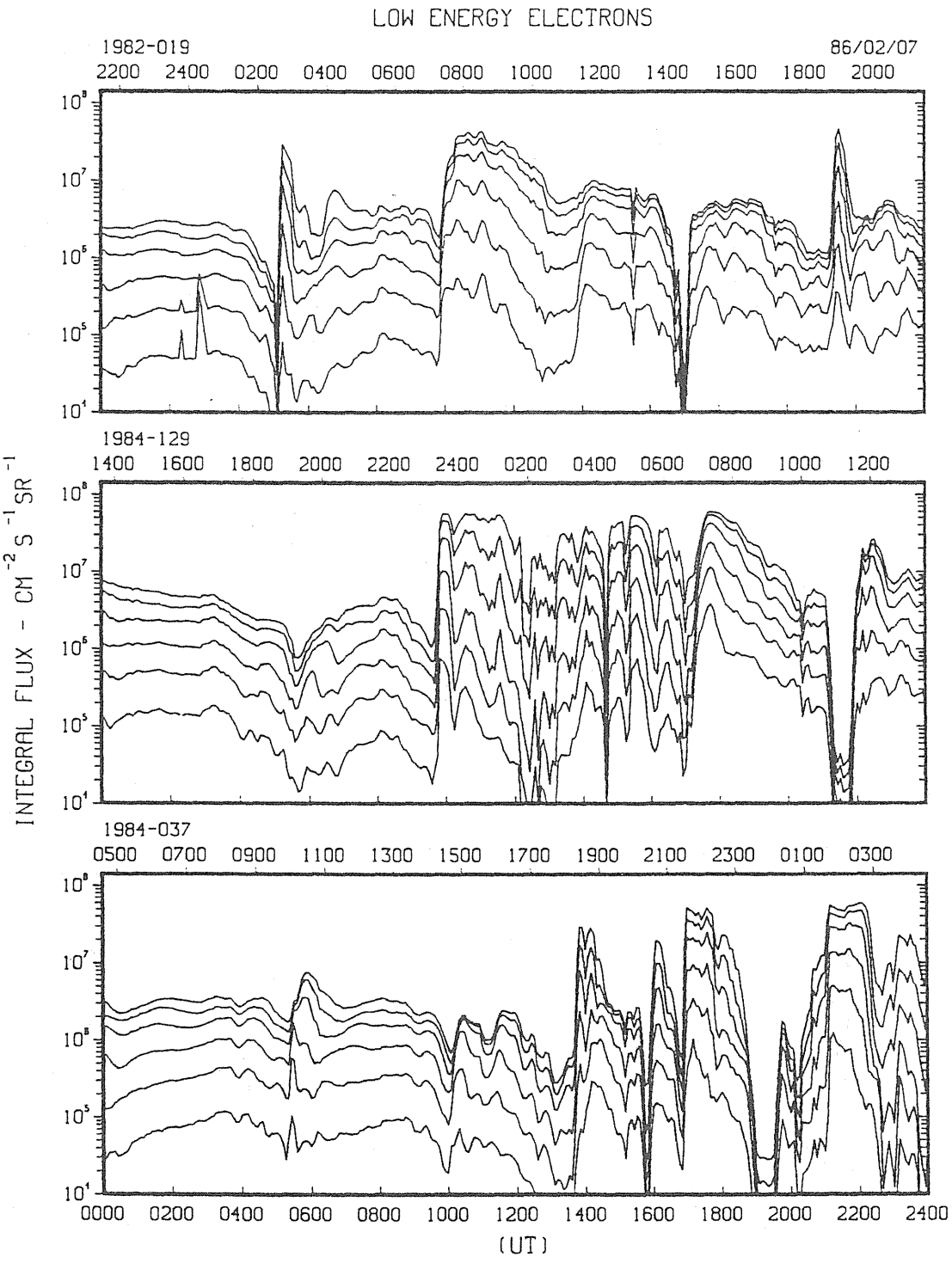
LOW ENERGY ELECTRONS
1982-019
86/02/07
2200 2400 0200 0400 0600 0800 1000 1200 1400 1600 1800 2000
1984-129
1400 1600 1800 2000 2200 2400 0200 0400 0600 0800 1000 1200
1984-037
0500 0700 0900 1100 1300 1500 1700 1900 2100 2300 0100 0300
INTEGRAL FLUX - CM -2 S -1 SR -1
0000 0200 0400 0600 0800 1000 1200 1400 1600 1800 2000 2200 2400
(UT)

Fig. 1a

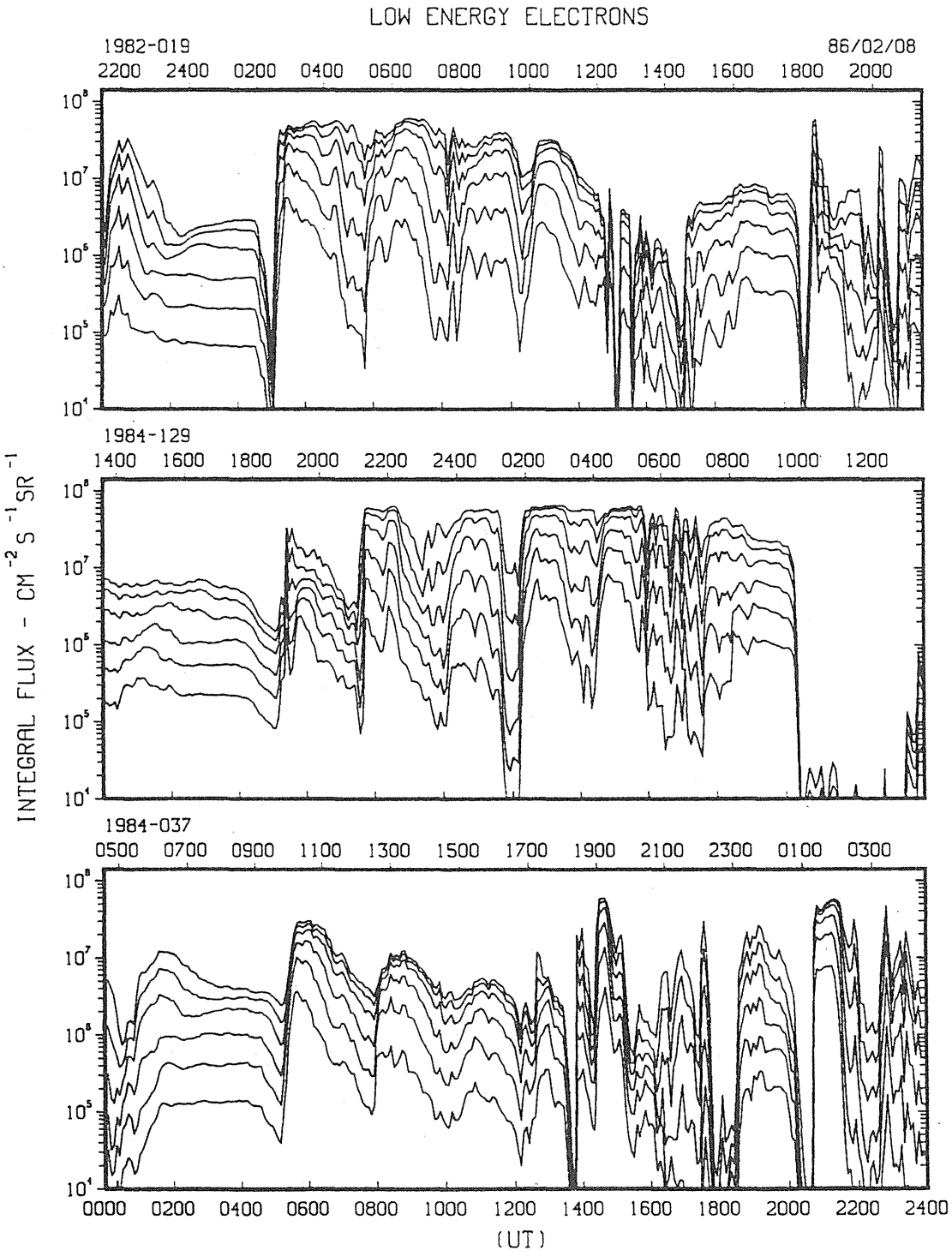
LOW ENERGY ELECTRONS
1982-019
86/02/08
2200 2400 0200 0400 0600 0800 1000 1200 1400 1600 1800 2000
1984-129
1400 1600 1800 2000 2200 2400 0200 0400 0600 0800 1000 1200
1984-037
0500 0700 0900 1100 1300 1500 1700 1900 2100 2300 0100 0300
INTEGRAL FLUX - CM^{-2} S^{-1} SR^{-1}
10^8
10^7
10^6
10^5
10^4
0000 0200 0400 0600 0800 1000 1200 1400 1600 1800 2000 2200 2400
(UT)

Fig. 1b

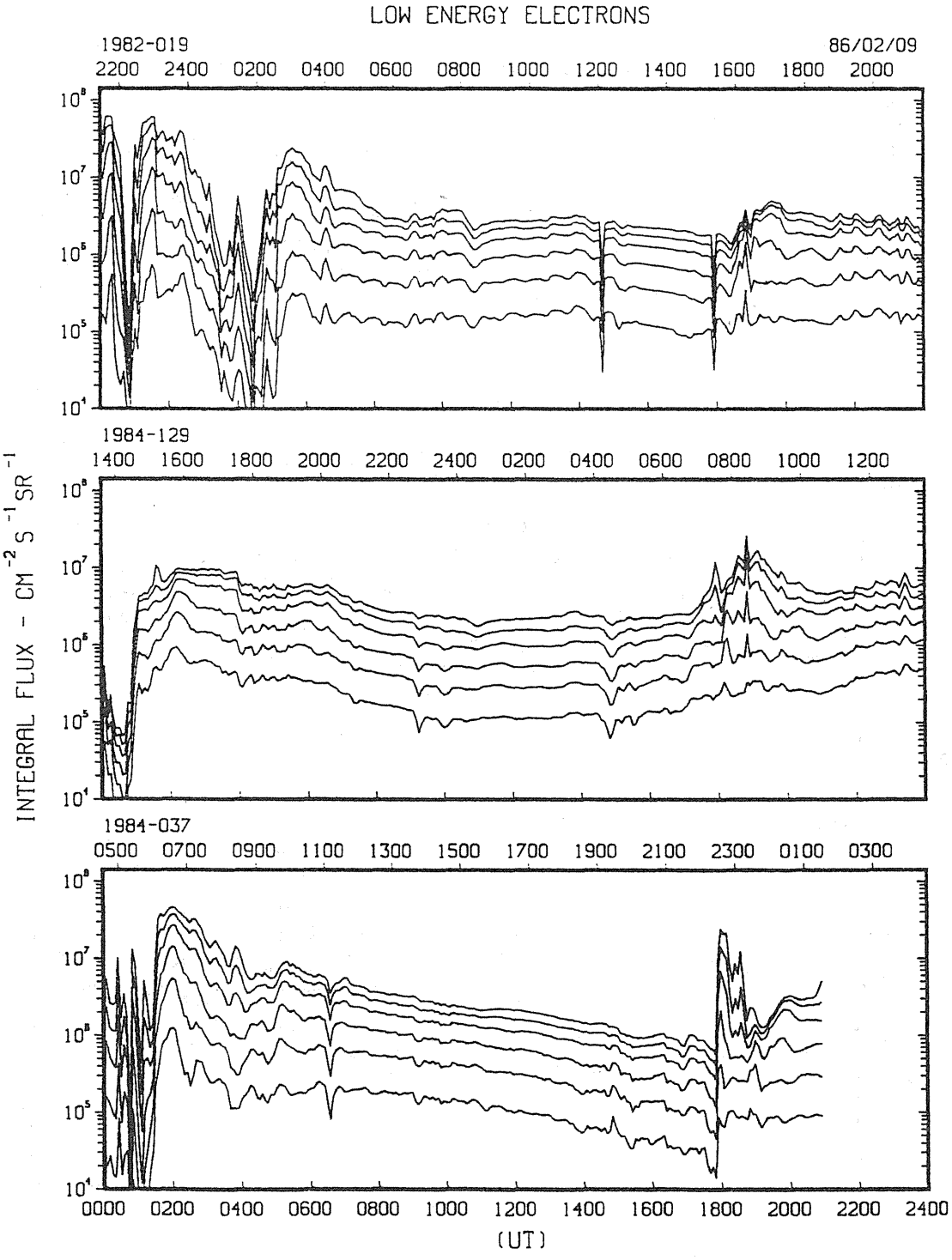
LOW ENERGY ELECTRONS
1982-019
86/02/09
2200 2400 0200 0400 0600 0800 1000 1200 1400 1600 1800 2000
1984-129
1400 1600 1800 2000 2200 2400 0200 0400 0600 0800 1000 1200
1984-037
0500 0700 0900 1100 1300 1500 1700 1900 2100 2300 0100 0300
INTEGRAL FLUX - CM -2 S -1 SR -1
0000 0200 0400 0600 0800 1000 1200 1400 1600 1800 2000 2200 2400
(UT)

Fig. 1c

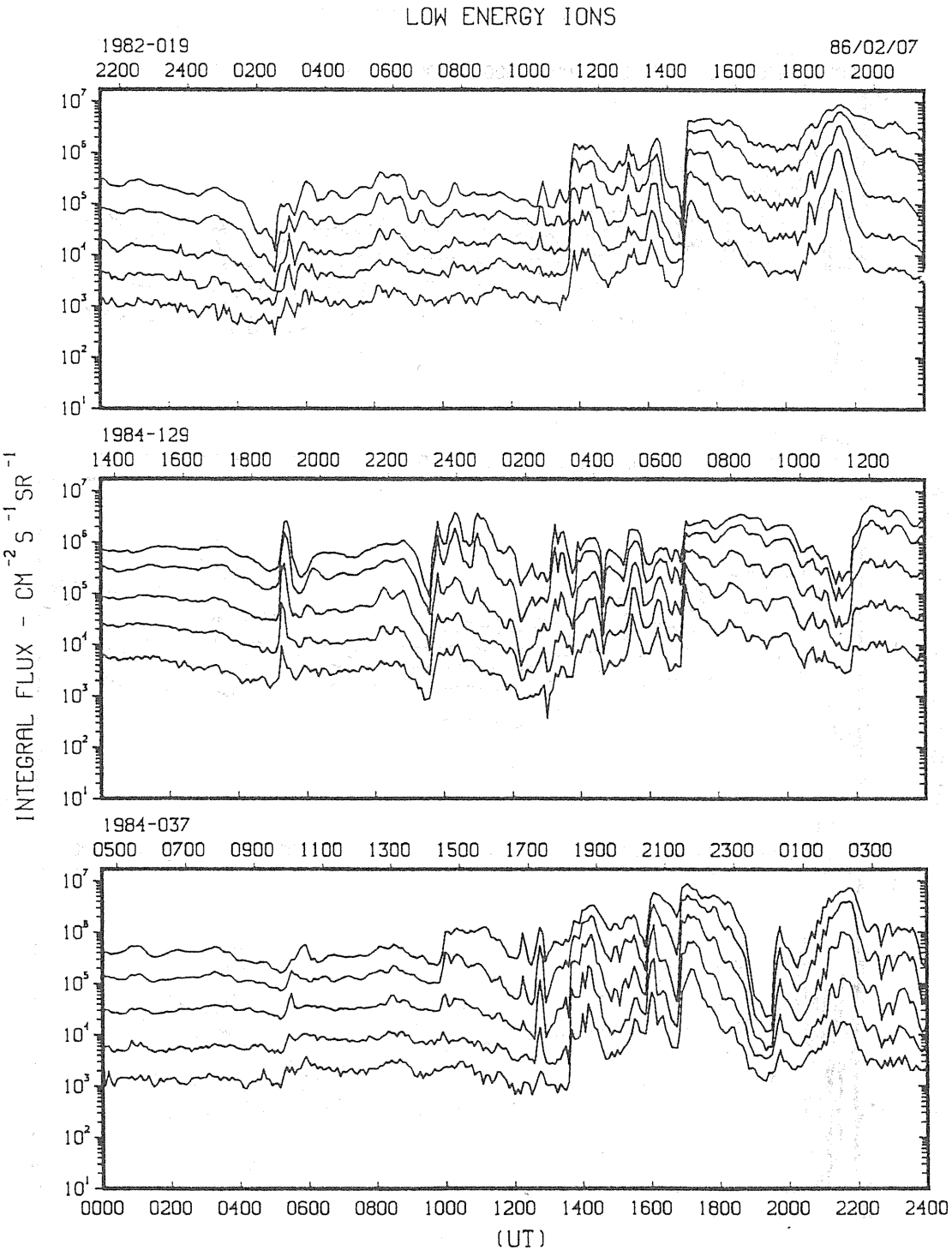
LOW ENERGY IONS
1982-019
86/02/07
2200 2400 0200 0400 0600 0800 1000 1200 1400 1600 1800 2000
1984-129
1400 1600 1800 2000 2200 2400 0200 0400 0600 0800 1000 1200
1984-037
0500 0700 0900 1100 1300 1500 1700 1900 2100 2300 0100 0300
INTEGRAL FLUX - CM^{-2} S^{-1} SR^{-1}
0000 0200 0400 0600 0800 1000 1200 1400 1600 1800 2000 2200 2400
(UT)

Fig. 2a

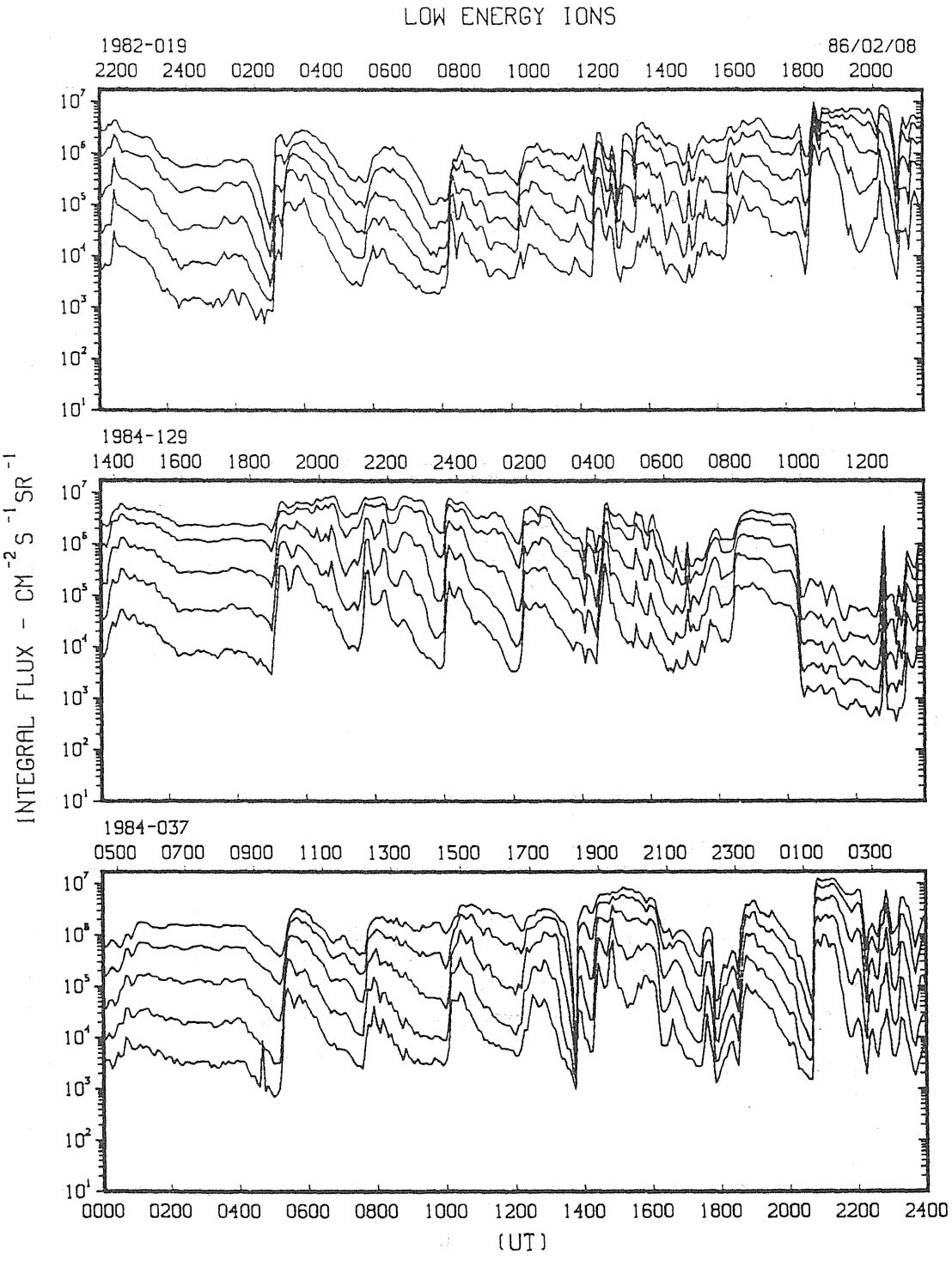
LOW ENERGY IONS
1982-019
86/02/08
2200 2400 0200 0400 0600 0800 1000 1200 1400 1600 1800 2000
1984-129
1400 1600 1800 2000 2200 2400 0200 0400 0600 0800 1000 1200
1984-037
0500 0700 0900 1100 1300 1500 1700 1900 2100 2300 0100 0300
0000 0200 0400 0600 0800 1000 1200 1400 1600 1800 2000 2200 2400
(UT)
INTEGRAL FLUX - CM^{-2} S^{-1} SR^{-1}

Fig. 2b

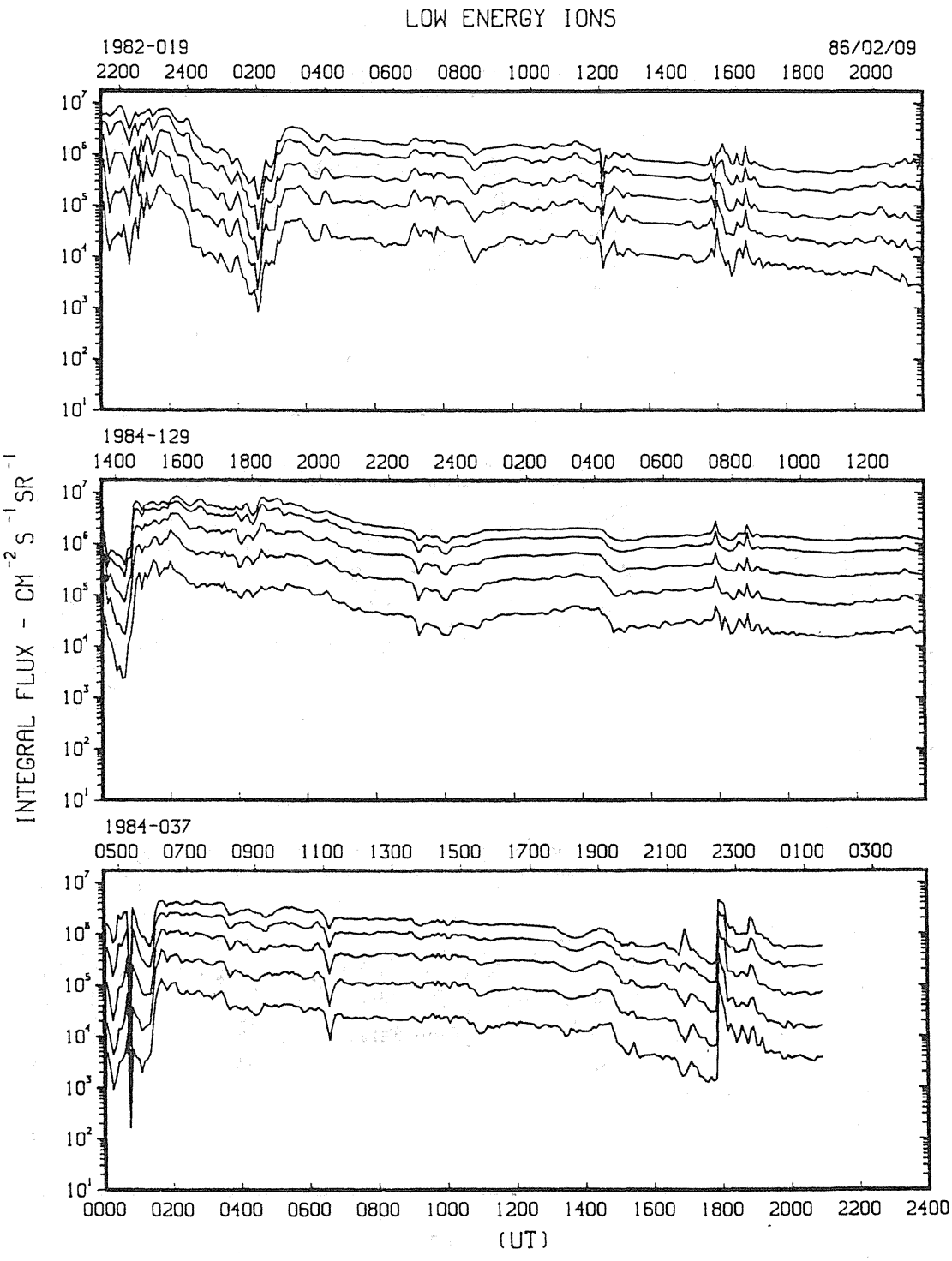
LOW ENERGY IONS
1982-019
86/02/09
2200 2400 0200 0400 0600 0800 1000 1200 1400 1600 1800 2000
1984-129
1400 1600 1800 2000 2200 2400 0200 0400 0600 0800 1000 1200
1984-037
0500 0700 0900 1100 1300 1500 1700 1900 2100 2300 0100 0300
INTEGRAL FLUX - CM -2 S -1 SR -1
0000 0200 0400 0600 0800 1000 1200 1400 1600 1800 2000 2200 2400
(UT)

Fig. 2c